Studies on Drying and Swelling of PAAm-NIPA Composites in Various Compositions

Gülşen Akın Evingür,[1] **Önder Pekcan**[2]
[1]*Physics Department, Istanbul Technical University, 34469, Maslak, Istanbul, Turkey*

[2]*Faculty of Arts and Science, Kadir Has University, 34083, Cibali, Istanbul, Turkey*

The steady-state fluorescence technique was introduced for studying the drying and swelling of disc-shaped PAAm-NIPA composites. Disc-shaped gels were formed with various acrylamides (AAm) and *N*-isopropylacrylamides (NIPA) by free radical crosslinking copolymerization in water. Composites were prepared with pyranine (*Py*) doped as a fluorescence probe. Scattered light, I_{sc}, and fluorescence intensities, *I*, were monitored during drying of these gels. The fluorescence intensity of pyranine increased and decreased as drying and swelling time increased respectively for all samples. The Stern-Volmer equation combined with moving boundary and Li-Tanaka models were used to explain the behavior of *I* during drying and swelling, respectively. It was found that the desorption coefficient, *D*, increased as NIPA contents were increased for a given temperature during drying. However, the cooperative diffusion coefficient, D_0, increased as NIPA contents were decreased during swelling at a given temperature. Supporting gravimetrical and volumetric experiments were also carried out during drying and swelling of PAAm-NIPA composites. It was observed that NIPA contents affect the drying and swelling process. POLYM. COMPOS., 32:928–936, 2011.

INTRODUCTION

Composites can be defined as a substance composed of two or more materials with different base structures combined in such a way that the end product has different properties than either of the parent materials [1]. Polyacrylamide (PAAm) can be polymerized easily by free radical crosslinking copolymerization (FCC) of AAm in the presence of *N*, *N*′-methylenebis (acrylamide) (BIS) as the crosslinker. An acrylamide-derived hydrogel can absorb solvent (water), but is itself insoluble. During water migration in the drying process, shrinkage corresponds simply to the compacting of the solid mass. These constitute a very important class of materials in food and cosmetics, as well as for biomedical or pharmaceutical applications [2]. On the other hand, poly(*N*-isopropylacrylamide), NIPA, is a well-known water soluble polymer with a lower critical solution temperature (LCST) at 31 to 35°C, and its network reveals unique thermal volume transitions near LCST [3]. Although the behavior of NIPA gel in aqueous solutions has been extensively investigated, a limited number of studies have been carried out concerning its behavior in a solid state. It is of particular interest whether the drying method can alter the physicochemical properties of the dried state of NIPA gel and thus influence its thermal-dependent behavior. Intermolecular interactions may occur mainly between NIPA molecules and water when the temperature is below the LCST, but when the temperature is above the LCST, NIPA molecules may aggregate in water as a result of both the intermolecular interactions within NIPA molecules and the hydrophobic interactions in the system [4].

Drying methods affect particle sizes, phase transitions, deswelling and reswelling processes, and the morphology of poly (*N*-isopropylacrylamide) microgel beads, as investigated by Lin et al. [4]. Hawlader et al. used a one-dimensional diffusion model to describe the heat and mass transfer in the wet and dry regions of materials undergoing shrinkage during drying [5]. Roques et al. investigated water diffusion and drying in polyacrylamide gels, proposing a mathematical model with independent parameters which analyzed the critical physical phenomenon [6]. A study based on the receding evaporating front model and on the assumption of a parabolic moisture content profile in the diffusion zone of the wet region has been conducted [7], in which it was observed that the experimental characteristic drying curve of plaster slabs was found to depend strongly on the thicknesses of the material. An excellent review of methods for processing the data obtained from drying kinetics was written by Kemp et al. [8], where different methods for fitting and smoothing drying curves are compared, with the aim of

Correspondence to: Önder Pekcan; e-mail: pekcan@khas.edu.tr
DOI 10.1002/pc.21111
Published online in Wiley Online Library (wileyonlinelibrary.com).

generating curves that can be used in industrial design. Scherer investigated the drying mechanisms of gels by diffusion [9] and shear modulus [10] and the status of the mechanism and practice of drying as stresses and cracking [11] was reviewed, with emphasis on work published [12]. A diffusive drying model for the drying of highly shrinkable materials like polyacrylamide gel and cellulosic paste has been reported [13], and recently, approximate models have been used by Coumans [14] to predict the drying kinetics for slab geometry. Wallqvist et al. studied the structural and thermodynamic properties of a water droplet enclosed in a spherical cavity embedded in a hydrophobic material [15].

The swelling kinetics of gels previously developed by Tanaka and Fillmore [16] and obtained from the kinetics of swelling agrees in terms of experimental accuracy with previous experiments by Peters and Candau [17]. The photon transmission technique was used to study the swelling of PAAm gels with various crosslinker contents [18, 19]. The decrease in transmitted light intensity, I_{tr}, was modeled using the Li-Tanaka equation from which the cooperative diffusion coefficients, D_0, were determined for various BIS content PAAm gels; the decrease in I_{tr} was attributed to lattice heterogeneities, which might have originated between microgels and holes in the swelling gel. We reported PAAm hydrogel swelling for various temperatures and crosslinker contents by using the steady state fluorescence (SSF) technique [20, 21]. It was observed that cooperative diffusion coefficients increased and decreased as the swelling temperature and crosslinker content was increased respectively. The transmitted light intensity, I_{tr}, from the gel increased in the initial stages when PAAm gels were immersed in water, and then decreased exponentially as the swelling time increased. The decrease in I_{tr} was modeled using the Li-Tanaka equation [22], and it was attributed to the lattice heterogeneities which might originate between "frozen blob clusters" and holes in the swelling gel [23]. On the other hand, the phase behavior of poly (*N*-isopropylacrylamide) has been extensively studied as a representative gel exhibiting nearly critical phase transition [24, 25]. The effect of preparation temperature on phase transitions of N-isopropylacrylamide gel was studied by Pekcan and Kara [26]. The results presented in this reference show that when the temperature is increased above the set temperature during the phase transition process, NIPA gel remembers its own heterogeneties which were gained during the gel formation process. Phase transitions of NIPA gels were prepared with various crosslinker contents [27], and the spinodal phase transition of NIPA gels was obtained by a suitable technique which could be used to study heterogeneous gel systems [27]. Recently, the fast transient fluorescence (FTRF) technique was used in our laboratory to study gel drying processes [28, 29]. Also, the SSF technique was employed to study the drying of polyacrylamide [30] at various temperatures and with various crosslinker contents [31].

Deuterium isotope effects on swelling–shrinking states of PAAm-PNIPA composites in aqueous solutions were investigated by using fluorescence spectroscopy. These effects in the microenvironment changes of PNIPA gel and polyacrylamide gel displayed similar characteristic [32]. The effect of hydrophobic monomer on the swelling behavior and mechanical properties of the present copolymeric hydrogels were showed [33]. Results presented that the equilibrium swelling ratio and critical gel transition temperature decreased with an increase of the hydrophobic monomer content.

The aim of this work was to investigate the drying and swelling process of PAAm-NIPA composites by using the steady-state fluorescence technique. By combining the Stern-Volmer equation with the moving boundary model desorption coefficients, D were determined for PAAm-NIPA composites during drying. The desorption coefficients, D increased as NIPA contents were increased. The Li-Tanaka equation was used to determine the swelling time constants, τ_1, and cooperative diffusion coefficients, D_0, for the swelling processes. It was observed that the swelling time constant, $\tau_{1,}$ increased and cooperative diffusion coefficients D_0 decreased as the NIPA contents increased at given temperatures. Gravimetrical and volumetric experiments also supported the results of the fluorescence measurements of PAAm-NIPA composites during drying and swelling processes.

THEORETICAL

Stern-Volmer Kinetics

This model is based on the variations of quantum yields of photophysical processes such as fluorescence, phosphoresce, and photochemical reactions with the content of a given quencher. The Stern-Volmer type of quenching mechanism can be proposed for the fluorescence intensity in the sample under consideration. According to the Stern-Volmer law, fluorescence intensity can be written as [34],

$$\frac{I_0}{I} = 1 + k_q \tau_0 [Q] \tag{1}$$

here, k_q is the quenching rate constant, τ_0 is the lifetime of the fluorescence probe with no quenching has taken place, and $[Q]$ is the quencher content and I_0 is the fluorescence intensity for the zero quencher content. This is referred to as the Stern-Volmer equation.

For low quenching efficiency, ($\tau_0\ k_q\ [Q] \ll 1$), *Eq. 1* becomes

$$I \approx I_0\big(1 - \tau_0 k_q [Q]\big) \tag{2}$$

If one integrates *Eq. 2* over the differential volume (dv) of the sample from the initial a_0 to final a_∞ thickness, then reorganization of the relation produces the following useful equation.

$$W = \int_{a_0}^{a_\infty} [W] d\upsilon \tag{3}$$

In our case, the amount of water diffusion, W is calculated over the differential volume by replacing Q with W as

$$W = \left(1 - \frac{I}{I_0}\right) \frac{\upsilon}{k_q \tau_0} \tag{4}$$

here it is assumed that water molecules are the only quencher for the excited pyranine molecules in our system, where υ is the volume at the equilibrium swelling state, which can be measured experimentally, k_q was obtained from separate measurements by using *Eq. 1* where the infinity equilibrium value of water diffusion, W, was used for each sample. Since τ_0 (=300 ns) is already known, then the measured values of I, W, and V at the equilibrium swelling condition can be used to calculate k_q for each swelling experiment separately.

Moving Boundary Model

The moving interface can be marked by a discontinuous change in content, as in the absorption by a liquid of a single component from a mixture of gases or by a discontinuity in the gradient of content as in the progressive freezing of a liquid [35]. When the diffusion coefficient is discontinuous at a content c, i.e. the diffusion coefficient is zero below c and constant and finite above c, then the total amount, M_t, of diffusing substance desorbed from the unit area of a plane sheet of thickness a at time t is given by the following relation

$$\frac{M_t}{M_f} = 2\left[\frac{D}{\pi a^2}\right]^{1/2} t^{1/2} \tag{5}$$

where D is a diffusion coefficient at content c_1. Here $M_f = ac_1$ is the equilibrium value of M_t. If one assumes that the diffusion coefficient of polymer segments in the gel is negligible compared to the desorption coefficient, D of water, then *Eq. 5* can be written as follows

$$\frac{W}{W_f} = 2\left[\frac{D}{\pi a^2}\right]^{1/2} t^{1/2} \tag{6}$$

here it is assumed that M_t is proportional to the amount of water molecules released, W, at time, t.

Li-Tanaka Model

The kinetics of the swelling of a gel is comprehensively described by the behavior of the displacement vector as a function of space and time. Li and Tanaka showed that the equation of motion is given by

$$f\frac{\partial \vec{u}}{\partial t} = \vec{\nabla}.\vec{\sigma} \tag{7}$$

where $\vec{u}$ is the displacement vector measured from the final equilibrium location after the gel is fully swollen ($\vec{u} = 0$ at $t = \infty$). The high value of the friction coefficient, f, between the network and solvent overdamps the motion of the network, resulting in a diffusion-like relaxation. σ_{ik} is the stress tensor. *Equation 7* was modified by Li and Tanaka and written as

$$\frac{\partial \vec{u}}{\partial t} = D_0 \nabla^2 u + \frac{K + \mu/3}{f} \vec{\nabla} \times (\vec{\nabla} \times \vec{u}) \tag{8}$$

where $D_0 = (K + 4\mu/3)/f$ is the collective diffusion coefficient. Here t denotes the time and K is the bulk modulus [36]. The total energy of a gel can be separated into bulk energy and shear energy. The bulk energy is related to the volume change, which is controlled by diffusion. The shear energy, on the other hand, can be minimized instantly by readjusting the shape of the gel [36]. As long as the shear modulus μ is not zero, the change of the total shear energy in response to any small change in shape that maintains constant volume element within the gel should be zero,

$$\delta F_{sh} = 0 \tag{9}$$

Each small diffusion process determined by *Eq. 8* must couple to a small shear process given by *Eq. 9*. Simultaneous solution of *Eqs. 8* and *9* produces the following equations for the swelling of a disc gel in axial and radial directions [36].

$$u_z(z,t) = u_z(z,\infty) \sum_n B_n e^{-t/\tau_n} \tag{10a}$$

$$u_r(r,t) = u_r(r,\infty) \frac{z}{a} \sum_n B_n e^{-t/\tau_n} \tag{10b}$$

where the axial and radial displacements are expressed as a series of components, each of them decaying exponentially with a time constant, τ_n. Here it is assumed that the swelling rates of a disc in the axial (z) and radial (r) directions are the same.

The first terms of the expressions are dominant at large t, that is, at the last stage of swelling. *Equation 10* can also be written in terms of water uptakes W and W_f at time t and equilibrium, respectively, as follows:

$$1 - \frac{W}{W_f} = \sum_{n=1}^{\infty} B_n \exp(-t/\tau_n) \tag{11}$$

In the limit of large t, or if τ_1 is much larger than the rest of τ_n, all higher terms ($n \geq 2$) in *Eq. 11* can be omitted and the swelling kinetics is given by the following relation

$$\frac{W}{W_f} = 1 - B_1 \exp(-t/\tau_1) \tag{12}$$

where B_1 is given by the following relation:

 DOI 10.1002/pc

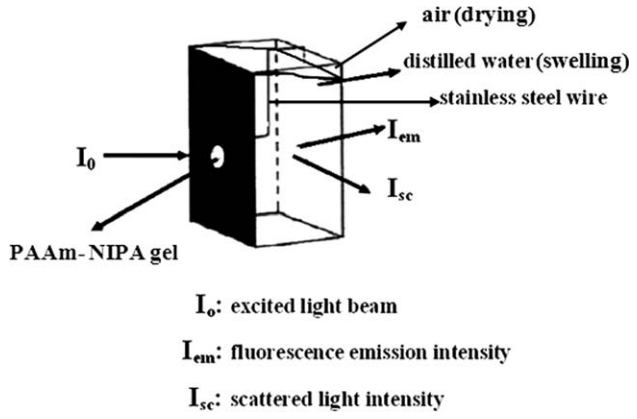

FIG. 1. The position of PAAm-NIPA composites in the fluorescence cell during drying (in air) and swelling (in water). I_0 is excitation, I_{em} is emission, and I_{sc} is scattered light intensities at 340 and 427 nm, respectively.

$$B_1 = \frac{2(3-4R)}{\alpha_1^2 - (4R-1)(3-4R)} \tag{13}$$

It should be noted from *Eq. 13* that $\sum B_n = 1$; therefore B_1 should be less than 1. B_1 is related to the ratio, R, of the shear modulus, μ and longitudinal osmotic modulus, $M = (K + 4\mu/3)$. Once the value of B_1 is obtained, one can determine the value of $R = \mu/M$. The dependence of B_1 on R for a disc [36] τ_1 is related to the cooperative diffusion coefficient, D_0, at the surface of a gel disc by

$$D_0 = \frac{3a_f^2}{\tau_1 \alpha_1^2} \tag{14}$$

where α_1 is a function of R only [36], and a_f stands for the half thickness of the gel in the final equilibrium state. Hence, D_0 can be calculated.

EXPERIMENTAL

Materials and Preparation of Composites

Composites were prepared with various molar percentages of PAAm and NIPA in distilled water at room temperature by keeping 2 M 0.01 g of BIS (*N*, *N*′-methylenebisacrylamide, Merck), 0.008 g of APS (ammonium persulfate, Merck) and 2 μl of tetramethylethylenediamine (TEMED, Merck) were dissolved in 5 ml distilled water (pH 6.5). *Py* content was kept constant at 4×10^{-4} M, for all experiments. The solution was stirred (200 rpm) for 15 min to achieve a homogenous solution. All samples were deoxygenated by bubbling nitrogen for 10 min just before polymerization process [37].

After drying these gels, swelling experiments of disc-shaped PAAm-NIPA composites were performed at various temperatures in water. The *Py* can be attached to the gel by Coulombic attractions [38]. *Py* content was kept constant at 4×10^{-4} M, for all experiments. The solution was stirred (200 rpm) for 15 min. to achieve a homogenous solution. All samples were deoxygenated by bubbling nitrogen for 10 min. just before the polymerization process. The drying and swelling experiments of

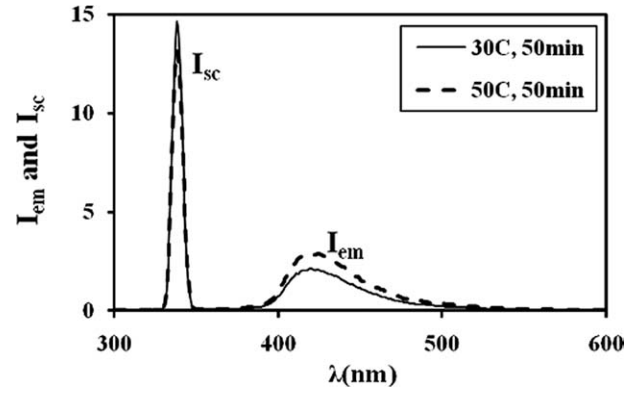

FIG. 2. Emission spectra of pyranine from the hydrogel prepared with 10 wt% NIPA content composites during the drying process. Each curve indicates the drying time at 30 and 50°C temperatures.

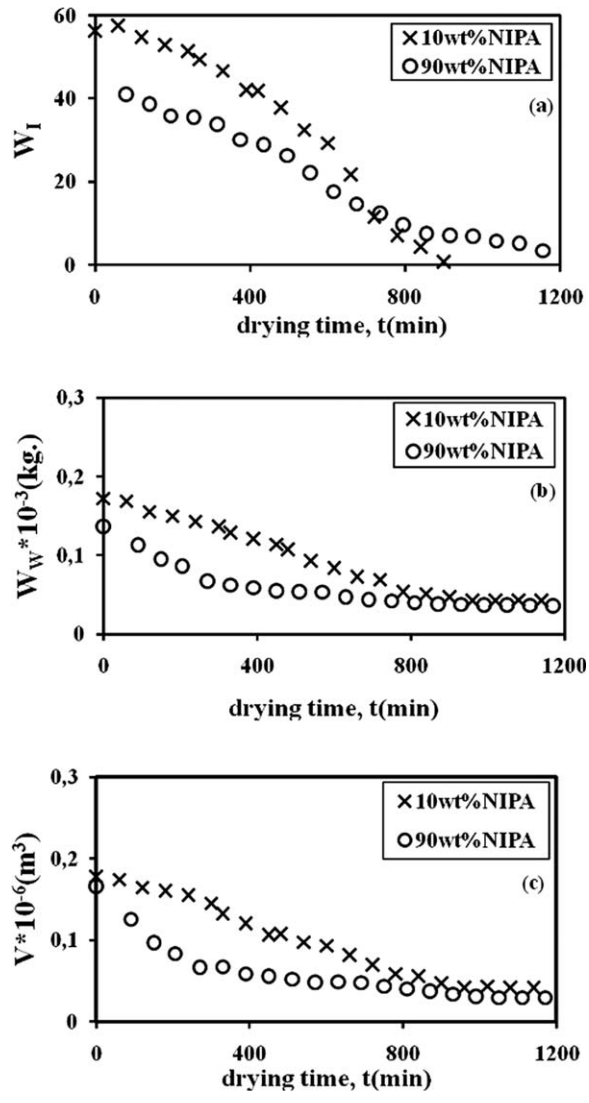

FIG. 3. The plots of water release, *W* measured by a) fluorescence, b) gravimetrical, and c) volumetric methods, versus drying time, *t*, for PAAm-NIPA composite gels dried in air at 20°C for 10 and 90 wt% NIPA content composites, respectively.

TABLE 1. Experimentally measured parameters of PAAm-NIPA composites for various NIPA contents and temperatures during drying processes.

T (°C)	wt% NIPA	$D_I \times 10^{-9}$ (m^2/s)	$D_W \times 10^{-9}$ (m^2/s)	$D_V \times 10^{-9}$ (m^2/s)
20	0	12.72	0.38	0.37
	10	39.45	0.41	0.96
	25	49.35	0.46	1.12
	50	63.27	0.58	1.27
	75	73.21	0.93	1.55
	90	85.45	1.01	1.58
	100	Opaque	1.02	1.61
30	0	14.10	1.29	0.45
	10	42.22	1.35	1.01
	25	76.79	2.08	1.35
	50	84.24	2.56	1.43
	75	93.30	3.73	1.89
	90	140.99	13.26	12.22
	100	Opaque	13.78	13.26
40	0	15	1.40	0.49
	10	46.81	2.37	1.37
	25	81.03	2.94	1.53
	50	104	3.01	1.66
	75	110.33	11.66	8.40
	90	125.85	11.91	8.75
	100	Opaque	12.34	8.86
50	0	26	3.40	1.58
	10	61.23	7.14	3.29
	25	103.40	8.55	4.81
	50	106.65	9.84	6.08
	75	108.86	10.54	7.96
	90	114.31	11.30	8.36
	100	Opaque	12.26	8.65
60	0	48.67	4.40	1.81
	10	52.30	5.44	2.47
	25	70.65	7.85	4.41
	50	98.48	8.03	5.68
	75	104.29	9.61	7.01
	90	110	11.24	8.26
	100	Opaque	12.16	8.40

disc-shaped PAAm-NIPA composites prepared with various (100 wt% PAAm, 90 wt% PAAm + 10wt% NIPA, 75 wt% PAAm % + 25 wt% NIPA, 50 wt% PAAm + 50 wt% NIPA, 25 wt% PAAm +75 wt% NIPA, 10 wt% PAAm + 90 wt% NIPA, 100 wt% NIPA) compositions were performed in air and in water, respectively at temperatures of 20, 30, 40, 50, and 60°C.

Fluorescence Measurements

The fluorescence intensity measurements were carried out using a Model LS-50 spectrometer from Perkin-Elmer, equipped with a temperature controller. All measurements were made at a 90° position and spectral bandwidths were kept at 5 nm. Disc-shaped gel samples were placed on the wall of a 1 cm path length square quartz cell filled with air and/or water for the drying and swelling experiments. Composites were excited at 340 nm during in situ experiments and emission intensities of the pyranine were monitored at 427 nm as a function of drying and swelling time. As the water released began to increase, the fluorescence intensity, I_{em}, increased and the scattered light intensity, I_{sc}, decreased. During swelling, however, I_{em} and I_{sc} behaved in an exact reverse manner to the drying behavior. The position of the PAAm-NIPA composite which was behind the hole in the cell and fixed by stainless steel wire and the incoming light beam for the fluorescence measurements are shown in Fig. 1 during the drying and swelling of the composite gel in the air and in distilled water. One side of the quartz cell was covered by black cardboard with a circular hole which was used to define the incoming light beam and limit its size to the dimensions of the gel disc. At the same time, a gravimetric measurement was performed by measuring weight. The distance and thickness of the PAAm-NIPA composite were also measured to calculate the volume of the PAAm-NIPA composite from the formula for a cylinder's volume.

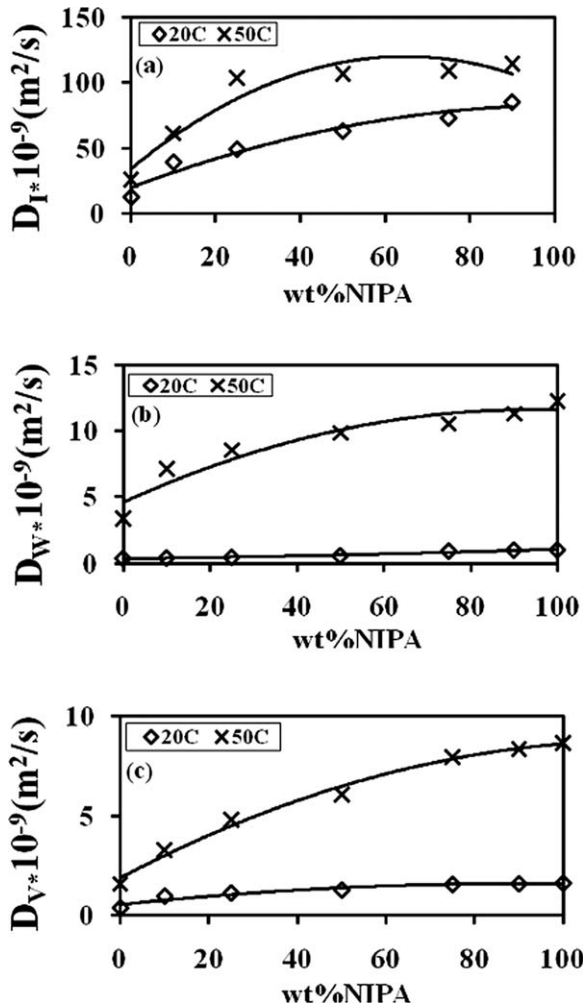

FIG. 4. Desorption diffusion coefficients versus NIPA content measured by a) fluorescence, b) gravimetrical, and c) volumetric techniques, measured at 20 and 50°C temperatures, respectively.

DOI 10.1002/pc

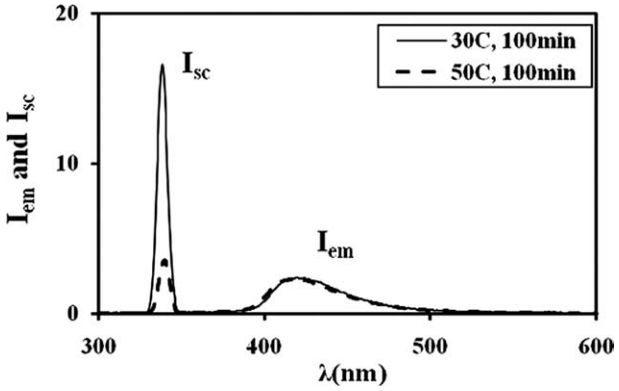

FIG. 5. Emission spectra of pyranine from the composite prepared with 10 wt% NIPA content samples during the swelling process. Each curve indicates the swelling time at 30 and 50°C different temperatures.

RESULTS AND DISCUSSION

Drying

Figure 2 shows the emission spectra of pyranine from the PAAm-NIPA composite during the drying process at 30 and 50°C for 10 wt% NIPA content. It can be seen in Fig. 2 that as the water release increases, fluorescence intensity, I_{em}, increases and the scattered light intensity, I_{sc}, decreases with the increasing temperature. Since the decrease in I_{sc} corresponds to the decrease in turbidity of the drying gel, the corrected fluorescence intensity, I, is defined as I_{em}/I_{sc}, i.e. as the drying time, t, is increased, the quenching of excited pyranines decreases due to an increase in the water release from the drying PAAm-NIPA composite. In order to quantify these results, a collisional type of quenching mechanism may be proposed for the fluorescence intensity, I, from the gel samples during the drying process by using *Eq. 4*. For the dry composite gel, τ_0 (=300 ns) is already known, so W can be calculated by using *Eq. 4* and the measured I values in each drying step. The plots of W versus t at various NIPA content samples are presented in Fig. 3a where the fit of the data to *Eq. 6* produced the desorption coefficient, D_I, which are listed in Table 1. D_I values increase by increasing the NIPA content at a given temperature which can be explained by the quick evaporation of the quencher (water) from the PAAm-NIPA composite system due to the low water-absorbing capacity of NIPA compared to PAAm. It is clear that lower NIPA-content gel dries more slowly, resulting in small D_I values in comparison to the high NIPA-content composite.

On the other hand, by using gravimetrical methods, water desorption was also measured from the drying PAAm-NIPA composite prepared at various NIPA contents. The plots of the data are presented in Fig. 3b at 20°C for 10 and 90 wt% NIPA content composites. The fits of water release, W versus $t^{1/2}$ to *Eq. 6*. for the various NIPA content composite dried at different temperatures produce the desorption coefficients, D_W, which are listed in Table 1, where it is observed that the desorption coefficient increases as the NIPA content is increased for each temperature, as discussed earlier. The variations in volume, V, of PAAm-NIPA composites during the drying process are also measured. The plots of the volume, V, versus drying time for 10 and 90 wt% NIPA content composites dried at 20°C is presented in Fig. 3c. The data in Fig. 3c is fitted to the following relation produced from *Eq. 6*.

$$\frac{V}{V_f} = 2\left(\frac{D}{\pi a^2}\right)^{1/2} t_d^{1/2} \tag{15}$$

here it is assumed that the relation between W and V is linear. Then using *Eq. 15*, the volumetric desorption coefficients D_V were determined and listed in Table 1. Again, it is seen that D_V values increased as the NIPA content increased at each temperature, similar to the D_W behavior. D_W and D_V coefficients are found to be much smaller in

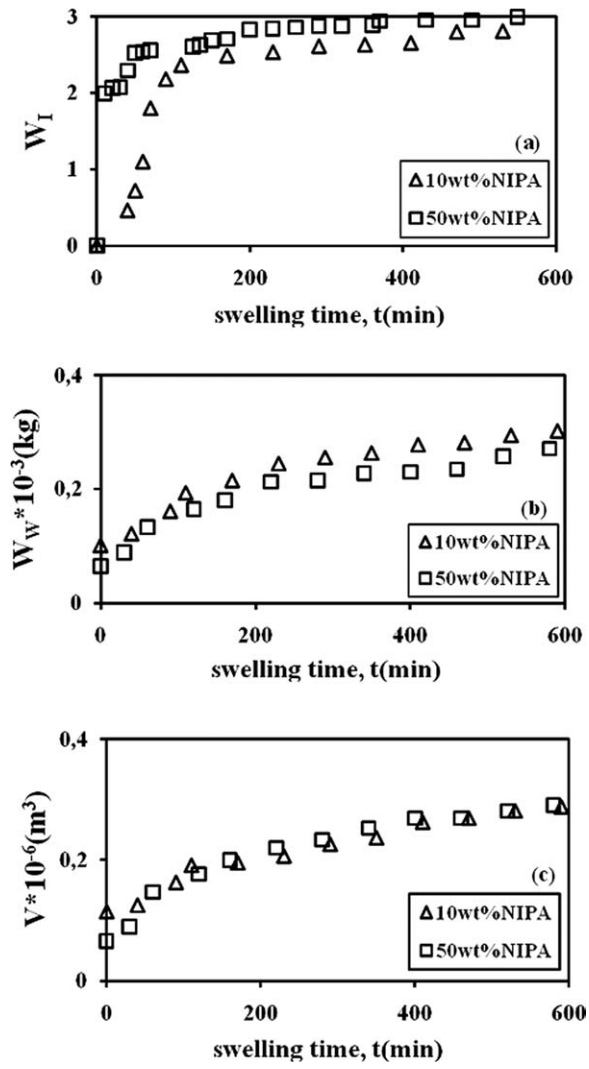

FIG. 6. The plots of water uptake, W measured by a) fluorescence, b) gravimetrical, and c) volumetric methods, versus swelling time, t, for PAAm-NIPA composites swollen in water at 20°C for 10, and 50 wt% NIPA content composites, respectively.

TABLE 2. Experimentally measured parameters of PAAm-NIPA composites for various temperatures and contents during swelling processes.

T (°C)	wt% NIPA	τ_{1I} (min)	$D_{0I} \times 10^{-9}$ (m^2/s)	τ_{1w} (min)	$D_{0w} \times 10^{-9}$ (m^2/s)	τ_{1v} (min)	$D_{0v} \times 10^{-9}$ (m^2/s)
20	10	76.92	1.45	223.9	1.51	200	2.31
	25	117.64	1.38	250	0.93	222.22	1.92
	50	181.81	0.74	270.27	0.91	243.9	1.89
	75	250	0.58	285.71	0.73	285.71	1.51
	90	270.27	0.42	303	0.63	312.5	0.54
	100		Opaque	307.69	0.60	318	0.52
30	10	90	1	232.55	1.42	212.76	1.95
	25	125	0.91	263.15	0.80	232.55	1.62
	50	250	0.65	285.71	0.74	250	1.51
	75	270.27	0.45	294.11	0.65	294.11	0.92
	90	370.37	0.25	333.33	0.25	333.33	0.25
	100		Opaque	338.98	0.217	338.98	0.08
40	10	153.84	0.92	256.41	0.82	243.9	1.33
	25	166.66	0.83	270.27	0.65	250	0.62
	50	270.27	0.49	289.01	0.58	263.15	0.59
	75	294.11	0.35	322.58	0.32	322.58	0.37
	90	285.71	0.32	322.58	0.46	322.58	0.33
	100		Opaque	333.33	0.35	333.33	0.25
50	10	200	0.52	263.15	0.54	250	0.67
	25	256.41	0.58	277.77	0.47	277.77	0.38
	50	294.11	0.46	294.11	0.45	307.69	0.44
	75	289.01	0.42	307.69	0.44	312.5	0.41
	90	294.11	0.37	312.5	0.48	312.5	0.40
	100		Opaque	325.73	0.37	325.73	0.37
60	10	171.42	0.67	235.84	0.55	232.55	0.83
	25	250	0.65	263.90	0.52	259.06	0.53
	50	270.27	0.60	263.15	0.48	285.71	0.48
	75	277.77	0.40	294.11	0.46	294.11	0.47
	90	285.71	0.38	307.69	0.50	307.69	0.46
	100		Opaque	325.73	0.45	325.73	0.45

high NIPA content gels, as was predicted earlier. Fig. 4a–c presents the desorption coefficients, D which were obtained from *Eq. 6* and *15*. and measured by fluorescence, gravimetric and volumetric techniques for 20 and 50°C content samples, respectively, where it was observed that the desorption coefficient increased as the NIPA content increased, as discussed earlier.

Swelling

Figure 5 shows the emission spectra of pyranine from the PAAm-NIPA composite during the swelling process at 30 and 50°C for 10 wt% NIPA content. Figure 5 presents the reverse behavior for I_{em} and I_{sc} during drying of thePAAm-NIPA composite. As the swelling time, t, increased, the quenching rate of excited pyranines increased due to water uptake. It should also be noted that quenching became more efficient at higher NIPA contents. In order to quantify these results, a collision type of quenching mechanism may be proposed for the fluorescence intensity, I, in the gel sample during the swelling process by using *Eq. 2*. For the swollen composite gel, if τ_0 (≈300 ns) is already known, then W can be calculated by using *Eq. 4* and the measured I values, at each step of the swelling [34]. Once the k_q values are measured, the water uptake, W, can be calculated from the measured τ_0 values in each step of the swelling. Here, it is assumed that the k_q values do not vary during the swelling processes, i.e. the quenching process solely originates from the water molecules. Plots of water uptake, W, versus swelling time are presented in Fig. 6a. The logarithmic form of the data in Fig. 6a was fitted to the following relation produced from *Eq. 12*

$$\ln\left(1 - \frac{W}{W_f}\right) = \ln B_1 - \frac{t}{\tau_{1I}} \tag{16}$$

here, τ_{1I} is the time constant, measured by the fluorescence technique and B_1 is related to the ratio of the shear modulus, μ and longitudinal osmotic modulus, M by *Eq. 13*. Using *Eq. 16* linear regression of the curves in Fig. 6a provided us with B_1 and τ_{1I} values. Taking into account the dependence of B_1 on R, one obtains R values and from the α_1-R dependence α_1 value was produced. The experimental determination of these values was based on the method described by Li and Tanaka [36]. Then, using *Eq. 14*, cooperative diffusion coefficients D_0 were determined for these disc-shaped gels and found to be around 10^{-9} m^2/s. Experimentally obtained τ_{1I} and D_{0I} values are summarized in Table 2. It should be noticed that D_{0I} values decreased as the NIPA content increased. As discussed above, the water absorbing capacity of NIPA is much lower than PAAm, which results in lower

 DOI 10.1002/pc

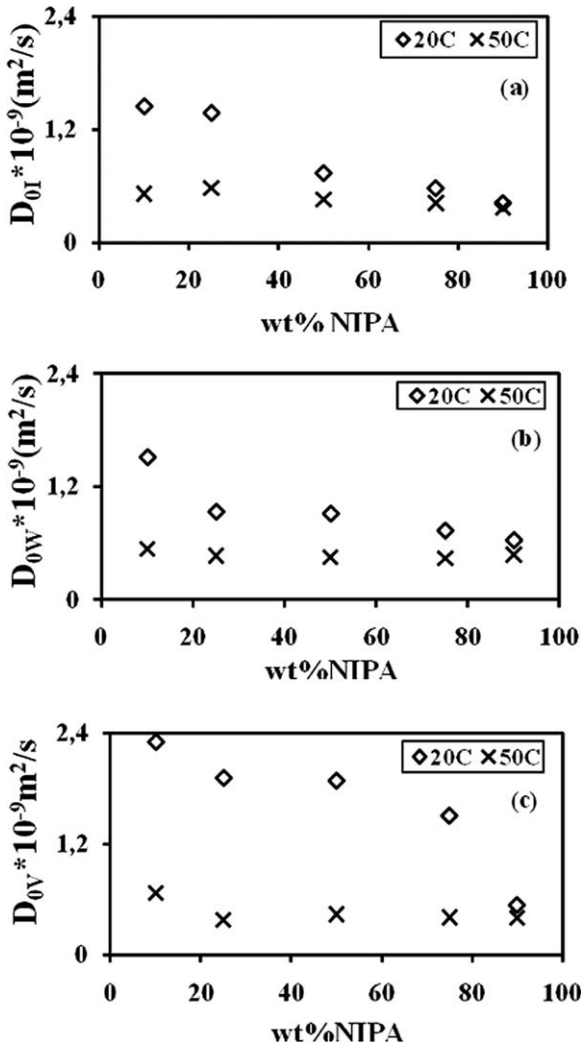

FIG. 7. Cooperative diffusion coefficients versus NIPA content measured by a) fluorescence, b) gravimetrical, and c) volumetric techniques, measured at 20 and 50°C temperatures, respectively.

swelling rates in a high NIPA-content composite. It is clear that lower-content NIPA gel swells more quickly in comparison to a high NIPA content composite.

The plots of the solvent uptake, W, versus swelling time measured gravimetrically at 20°C for 10 and 50 wt% NIPA content composite swollen in water are shown in Fig. 6b. These are typical solvent uptake curves, obeying the Li-Tanaka equation, *Eq. 12*. The logarithmic forms of the data in Fig. 6b were fitted to the following relation produced from *Eq. 12*,

$$\ln\left(1-\frac{W}{W_f}\right)=\ln B_1-\frac{t}{\tau_{1w}} \tag{17}$$

from which B_1 and the gravimetric time constant, τ_{1w} were determined. Then, using *Eq. 14*, gravimetric cooperative diffusion coefficients D_{0w}, were determined and are listed in Table 2 with the τ_{1w} values. A similar decrease in D_{0w} as for D_{0I} was observed as the NIPA contents were increased at the given temperatures. The variations in the volume, v, of the PAAm-NIPA composites during the swelling process were also measured. The plots of the volume, v, versus swelling time for PAAm-NIPA composites swollen in water are presented in Fig. 6c, which is again typical solvent uptake curves, obeying the Li-Tanaka equation, *Eq. 12*. The logarithmic forms of the data in Fig. 6c were fitted to the following relation produced from *Eq. 12*.

$$\ln\left(1-\frac{v}{v_f}\right)=\ln B_1-\frac{t}{\tau_{1v}} \tag{18}$$

from which B_1 and τ_{1v} were determined. Here, it is assumed that the relation between W and v was linear. Then using *Eq. 14* the volumetric cooperative diffusion coefficients, D_{0v}, were determined and are listed in Table 2. Again, it is seen that the D_{0v} values decreased as the NIPA content increased at each temperature, similar to D_{0W} behavior. In summary, D_0 values were found to be smaller in high NIPA content composites as shown in Fig. 7. This is because these gels swell much more slowly than low NIPA composites. In other words, the presence of NIPA in the PAAm gel creates smaller water absorbing volumes, which then result in slower swelling in high NIPA-content composites.

CONCLUSION

This study has demonstrated that the fluorescence method can be used to monitor the drying and swelling behaviors of PAAm-NIPA composites prepared with various NIPA contents and measured at different temperatures. A moving boundary model combined with Stern-Volmer kinetics was used to measure the desorption coefficients, D, for drying processes. It was observed that high NIPA content composites dry much more quickly as the result of having larger D coefficients for all measurements compared with low NIPA-content composites. A similar fluorescence method was employed to measure the swelling time constants, τ_1, and cooperative diffusion coefficients, D_0, for composite samples prepared with various NIPA content. The Li-Tanaka Model combined with Stern-Volmer kinetics was used to measure the cooperative diffusion coefficients for the swelling process at different temperatures. The results were interpreted in terms of the swelling time constants; τ_1 (increased) and D_0 (decreased) as the NIPA content increased. It was observed that high NIPA content composites swell much more slowly as the result of having smaller D_0 coefficients for all measurements in comparison to low NIPA content composites for a given temperature.

REFERENCES

1. K. Friedrich, S. Fakinov, and Z. Zhang, *Polymer Composites from Nano- to Macro-Scale*, Springer, New York (2005).

2. S.S. Waje, M.W. Meshram, V. Chaudhary, R. Pandey, P.A. Mahanawar, and B.N. Thorat, *Braz. J. Chem. Eng*., **22**(**02**), 209 (2005).
3. Y. Ono and T. Shikata, *J. Phys. Chem. B*, **111**(**7**), 1511 (2007).
4. S.Y. Lin, K.S. Chen, and L.R. Chu, *Polymer*, **40**, 6307 (1999).
5. M.N.A. Hawlader, J.C. Ho, and Z. Qing, *Dry. Technol*., **17**(**1–2**), 27 (1999).
6. M.A. Roques, F. Zagrouba, and P.D. Sobral, *Dry. Technol*., **12**(**6**), 1245 (1994).
7. L. Derdour, H. Desmorieux, and J. Andrieu, *Dry. Technol*., **18**(**1–2**), 237 (2000).
8. I.C. Kemp, B.C. Fyhr, S. Laurent, M.A. Roques, C.E. Groenewold, E. Tsotsas, A.A. Sereno, C.B. Bonazzi, and J.J. Bimbenet, *Dry. Technol*., **19**(**1**), 15 (2001).
9. W.G. Scherer, *J. Non-Cryst. Solids*, **107**, 135 (1989).
10. W.G. Scherer, *J. Non-Cryst. Solids*, **109**, 183 (1989).
11. W.G. Scherer, *J. Non-Cryst. Solids*, **147–148**, 363 (1992).
12. W.G. Scherer, *J. Non-Cryst. Solids*, **109**, 171 (1989).
13. W. Jomma, W. Aregra, J.R. Puiggali, and M. Quintard, *Dry. Technol*., **9**, 110 (1991).
14. W.J. Coumans, *Chem. Eng. Process*., **39**, 53 (2000).
15. A. Wallqvist, E. Gallicchio, and R.M. Levy, *J. Phys. Chem. B*, **105**, 6745 (2001).
16. T. Tanaka and D. J. Fillmore, *J. Chem. Phys*., **70**(3), 1214 (1979).
17. A. Peters and S.J. Candau, *Macromolecules*, **19**(7), 1952 (1986).
18. Ö. Pekcan and S. Kara, *Polym. Plast. Technol. Eng*., **41**(3), 573 (2001).
19. Ö. Pekcan and S. Kara, *Polymer*, **42**, 10045 (2001).
20. D. Kaya Aktaş, G. Akın Evingur, and Ö. Pekcan, *J. Mater. Sci*., **42**, 8481 (2007).
21. D. Kaya Aktaş, G. Akın Evingur, and Ö. Pekcan, *Adv. Polym. Technol*., **28**(**4**), 215 (2009).
22. Ö. Pekcan and S. Kara, *J. Appl. Polym. Sci*., **82**, 894 (2001).
23. Ö. Pekcan and S. Kara, *Polymer*, **41**, 8735 (2000).
24. T. Okajima, I. Harada, K. Nishio, and S. Hirotsu, *J. Chem. Phys*., **116**(**20**), 9068 (2002).
25. R.O.R. Costa and R.F.S. Freitas, *Polymer*, **43**, 5879 (2002).
26. Ö. Pekcan and S. Kara, *Phase Transitions*, **76**(**6**), 601 (2003).
27. S. Kara and Ö. Pekcan, *Mater. Chem. Phys*., **80**, 555 (2003).
28. M. Erdogan and Ö. Pekcan, *Compos. Interfaces*, **10**(**6**), 547 (2003).
29. M. Erdogan and Ö. Pekcan, *Polymer*, **45**, 2551 (2004).
30. D. Kaya Aktaş, G. Akın Evingür, and Ö. Pekcan, *J. Macromol. Sci. Phys*., **46**, 581 (2007).
31. G. Akın Evingür, D. Kaya Aktaş, and Ö. Pekcan, *Chem. Eng. Process*, **48**, 600 (2009).
32. H. Shirota, K. Ohkawa, N. Kuwabara, N. Endo, and K. Horie, *Macromol. Chem. Phys*., **201**(**16**), 2210 (2000).
33. W. Lee and Y. Yeh, *Eur. Polym. J*., **41**, 2488 (2005).
34. J.B. Birks, *Photopyhsics of Aromatic Molecules*, Wiley, Interscience, New York (1971).
35. J. Crank, *The Mathematics of Diffusion*, Clarendon Press, Oxford (1975).
36. Y. Li and T. Tanaka, *J. Chem. Phys*., **92**, 1365 (1990).
37. G. Akın Evingür, D. Kaya Aktaş, and Ö. Pekcan, *Phase Transitions*, **82**(**1**), 53 (2009).
38. Y. Yılmaz, N. Uysal, A. Gelir, O. Güney, D. Kaya Aktaş, S. Göğebakan, and A. Öner, *Spectrochim. Acta Part A*, **72**, 332 (2009).

 DOI 10.1002/pc